Science Advances
AAAS

Supplementary Materials for

Self-adaptive virtual microchannel for continuous enrichment and separation of nanoparticles

Yang Yang *et al.*

Corresponding author: Xuexin Duan, xduan@tju.edu.cn

Sci. Adv. **8**, eabn8440 (2022)
DOI: 10.1126/sciadv.abn8440

The PDF file includes:

Figs. S1 to S13
Table S1
Legends for movies S1 to S11

Other Supplementary Material for this manuscript includes the following:

Movies S1 to S11

Supplementary Figures

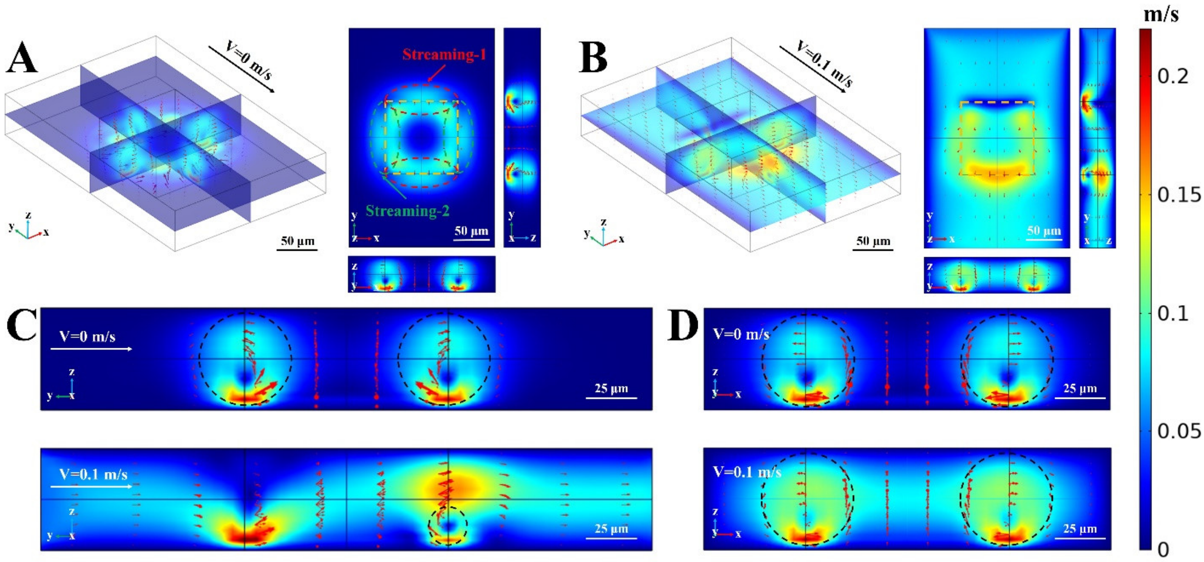

Fig. S1. Three dimensional simulation results of acoustic streaming induced by GHz square acoustic device. The three dimensional morphologies of both perpendicular (Streaming-1) and parallel (Streaming-2) acoustic streaming in static state (A) and lateral flow state (B). The outline of acoustic device is highlighted by a square dashed rectangle and the perpendicular and parallel streaming are represented by red and green dashed ovals. The slice diagrams show the distribution of streaming vortices in z-y plane (C) and x-z plane (D) in the lateral flow of 0 and 0.1 m/s, respectively. The action zones of acoustic streaming are shown by black dashed cycles.

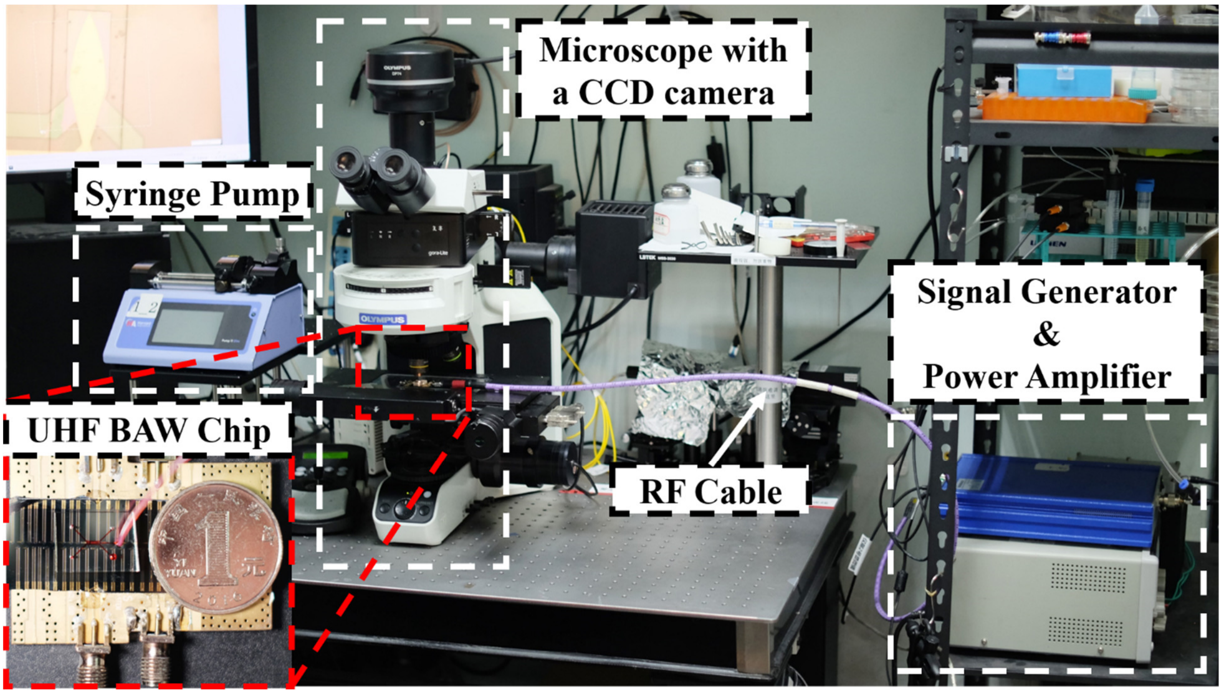

Fig. S2. The photo of System setup. The system of the virtual microchannel platform can be divided into four parts, including the RF actuating, fluid drive, observation modules and the UHF BAW chip. The RF actuating module contains the signal generator and the power amplifier, which is connected with UHF BAW chip by a RF cable. The fluid drive module is consisted by a set of syringe pumps. The observation module is a fluorescent microscope with a CCD camera. The UHF BAW chip consists of a UHF BAW device covered with microfluidic channel. The UHF BAW device is connected with the printed circuit board by wire bond, then connected with RF cable by the SMA connector.

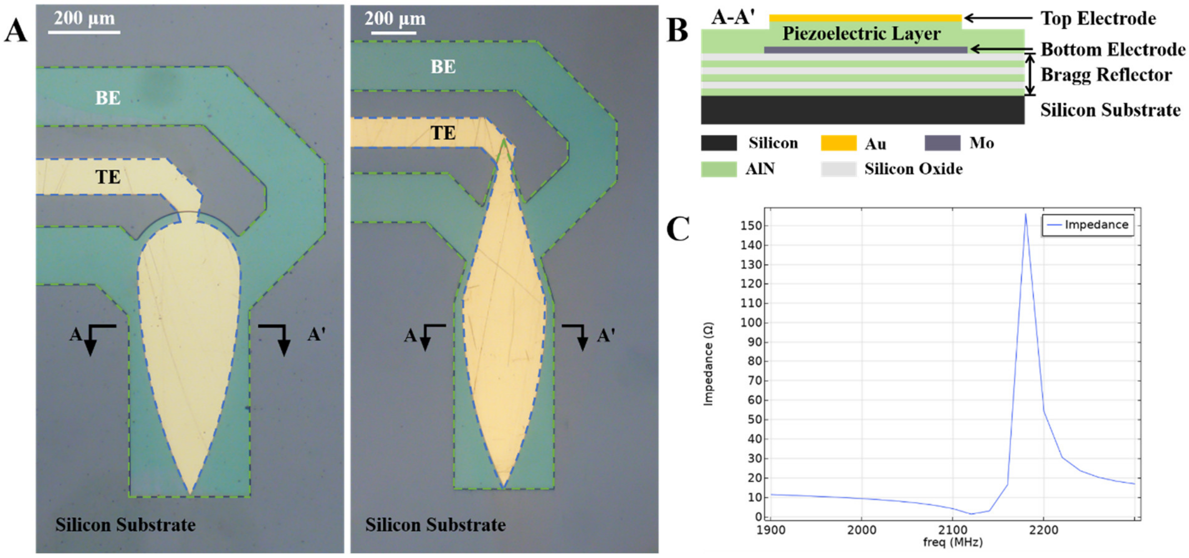

Fig. S3. Characteristics of the GHz BAW device. (A) The images of the GHz BAW device. The bottom and top electrodes (BE and TE) are represented by green and blue dashed lines (B) Section view of the GHz BAW device. The structures from bottom to top are a silicon substrate, a Bragg reflector, a bottom electrode (BE), a piezoelectric layer and a top electrode (TE). (C) The simulation result of the frequency response shows that the parallel resonant frequency of the GHz BAW device is higher than 2 GHz. The scale bar is 200 µm.

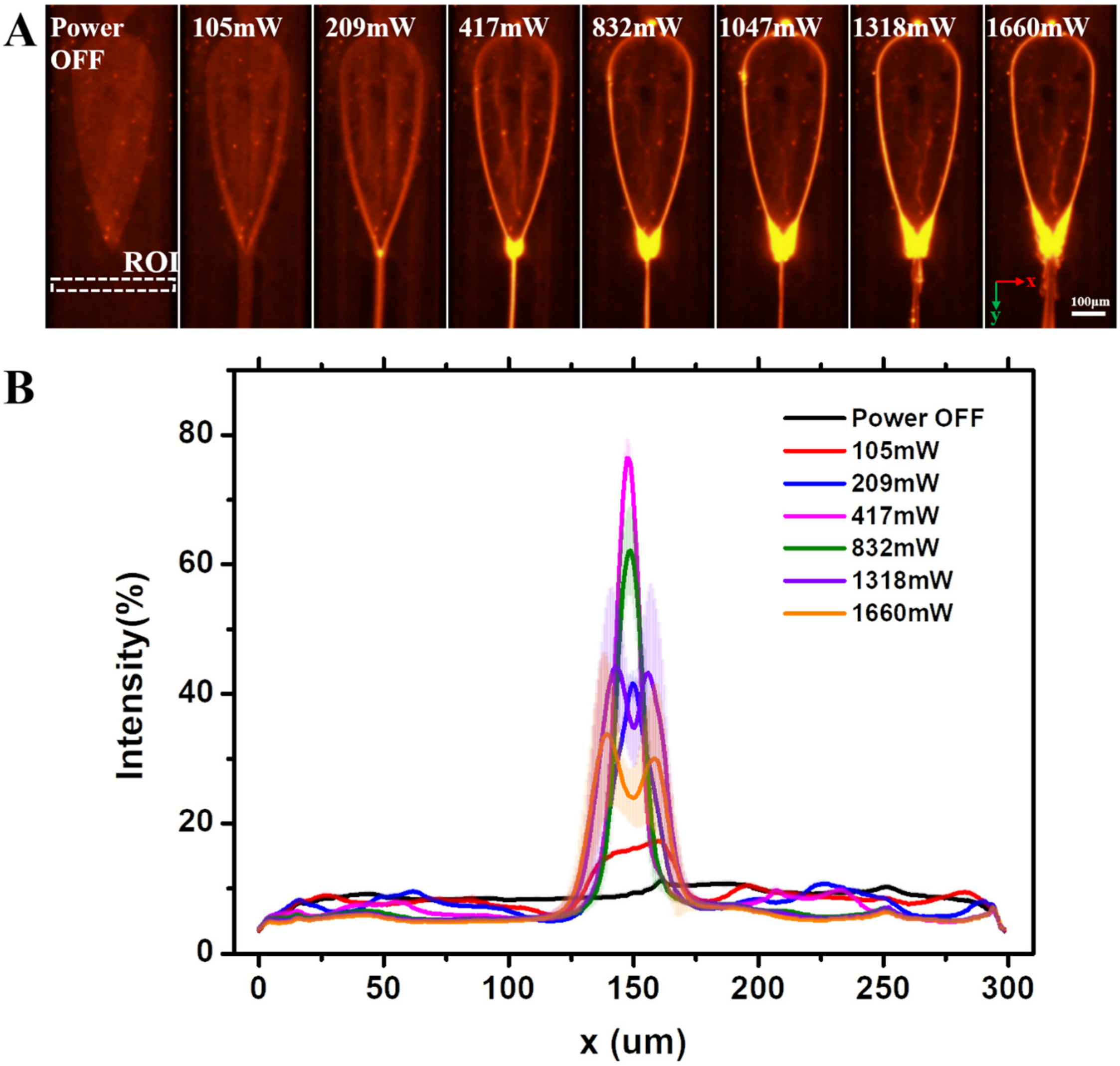

Fig. S4. Continuously enriched nanoparticles at different applied powers. (A) Images of continuous focusing of fluorescent nanoparticles (300 nm) via a focusing-type GHz BAW device at different applied powers. The lateral flow rates were 1 μL/min. (B) The efficiency of nanoparticle enrichment via stereo acoustic streaming is determined by the normalized image intensity of the region of interest (ROI). The efficiency of the enrichment first increases and then decreases with increasing power. Each curve was extracted and calculated from 10 discrete images. The scale bar is 100 μm.

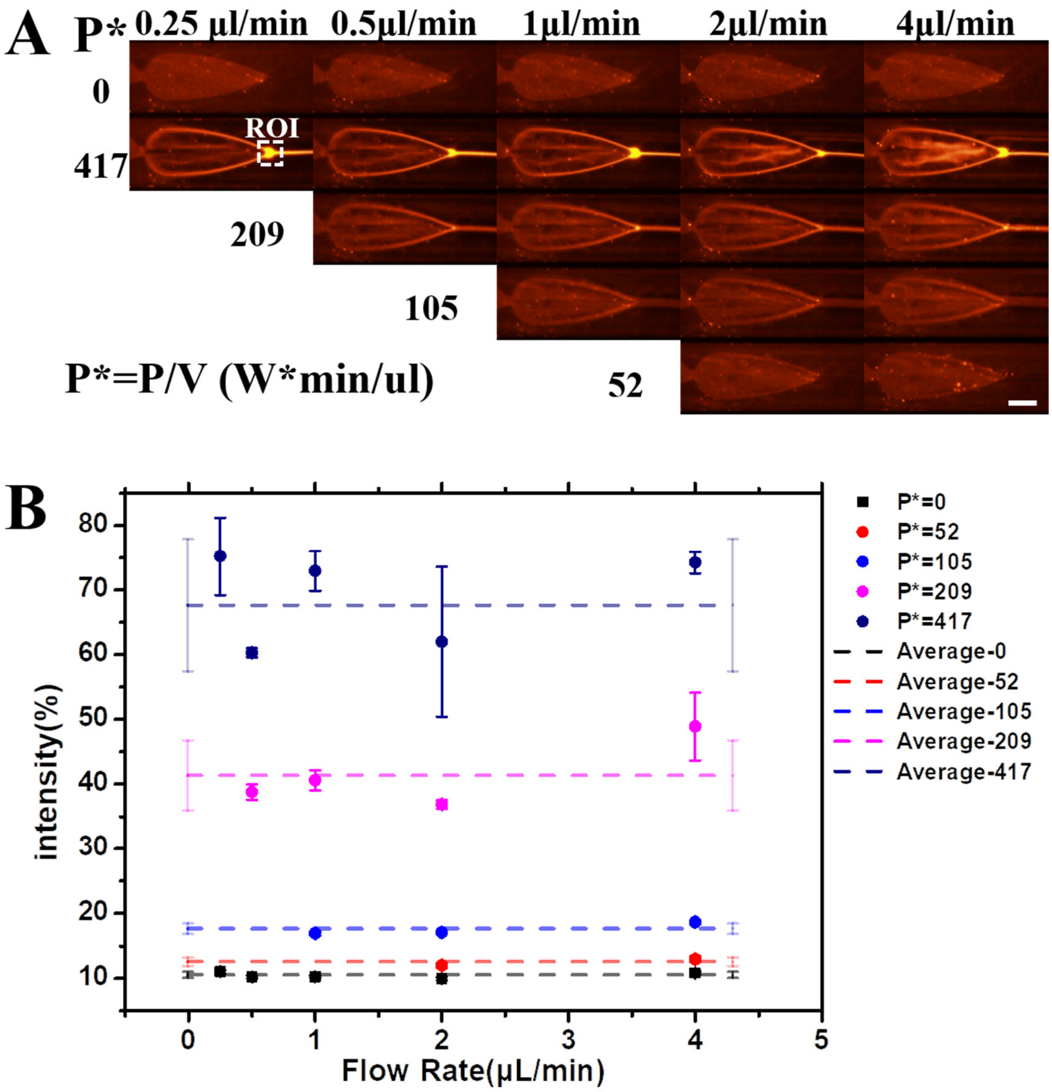

Fig. S5. Focusing morphology as a function of P*. (A) Images of continuous focusing of fluorescent nanoparticles (300 nm) via a focusing-type GHz BAW device at different P* and flow rates. Equivalent phenomena can be produced at arbitrary powers and lateral flow conditions by maintaining the ratio between the applied power and the lateral flow rate. (B) The enrichment efficiency of stereo acoustic streaming is defined by the highest normalized image intensity in the ROI. The enrichment efficiency was nearly the same at various flow rates. The dotted lines represent the average value in the same P*. Each dot was calculated from 10 discrete images. P and V represent the applied power and the lateral flow rate, respectively. The scale bar is 100 µm.

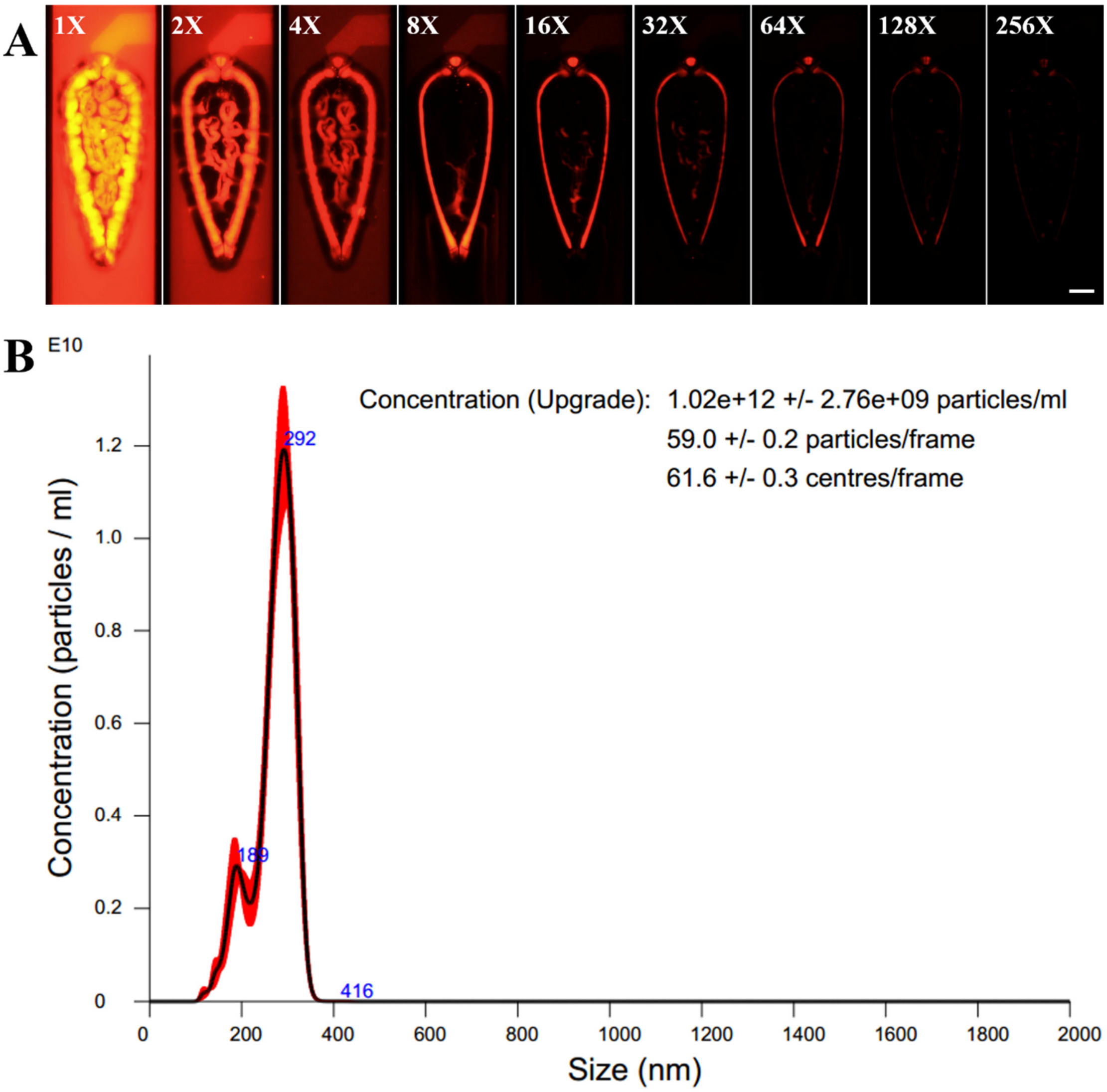

Fig. S6. In situ enrichment of nanoparticles at different concentrations. (A) Fluorescence images of nanoparticle enrichment at different concentrations without lateral flow. The diameter of the PS nanoparticles was 300 nm. The scale bar is 100 µm. (B) The size distribution and concentration of the 300-nm PS particles characterized by NTA.

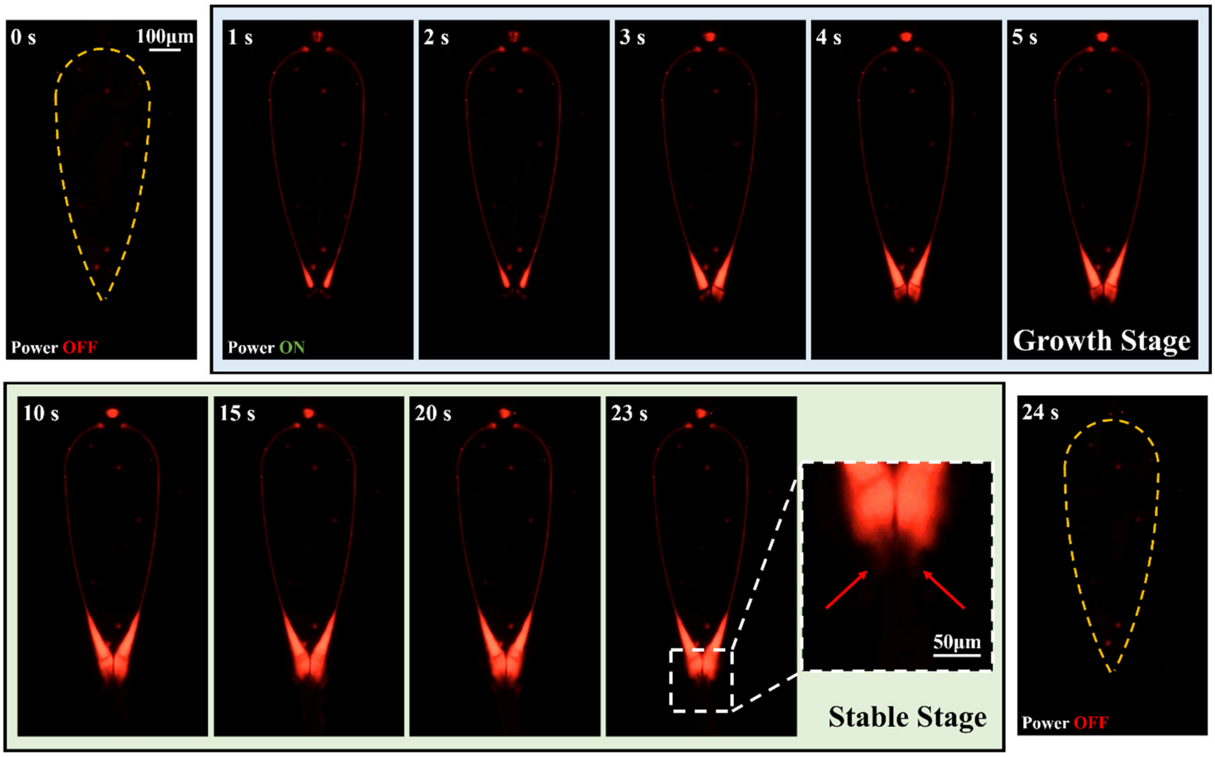

Fig. S7. Process of in-situ enrichment. The different moments of the enrichment process are shown and the time is indicated in the upper left corner. The 256x diluted 300-nm PS nanoparticle were injected into the microfluidic channel. When the device is turned on, the nanoparticles are focused by the virtual microchannel and migrated to the apex of the device. The total amount of enriched nanoparticles increases with time until the upper limit of the virtual microchannel's capacity is reached, this phase is called the growth stage highlighted by a blue rectangle. Subsequently, the enrichment entered a stable stage represented by the green rectangle, and the upstream particles were continuously captured, while the downstream particles were continuously scattered, and the two process maintaining the dynamic balance of the enrichment. The scattered nanoparticles are pointed by the red arrows in the detail image. The UHF device before and after are shown in the image at 0 s and 24 s and the outline of device is represented by the yellow dashed arc.

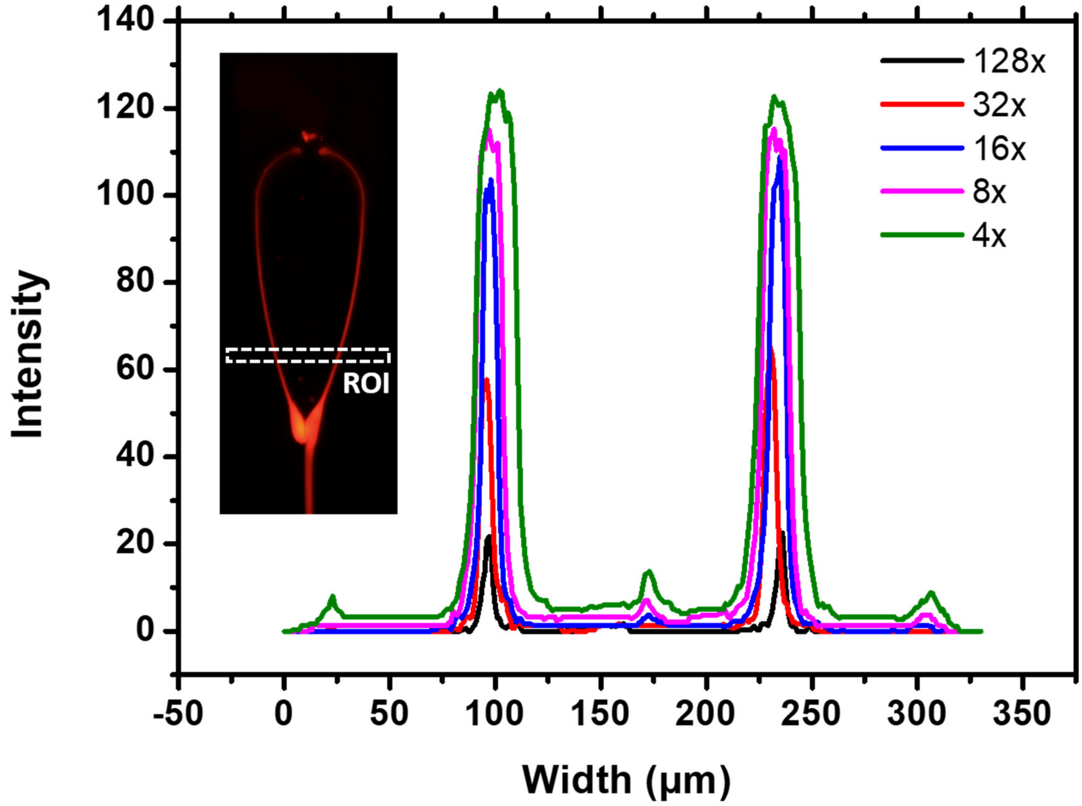

Fig. S8. Representation of the virtual channel with different sample concentrations. The ROI is shown in the image and highlighted by a white dashed rectangle.

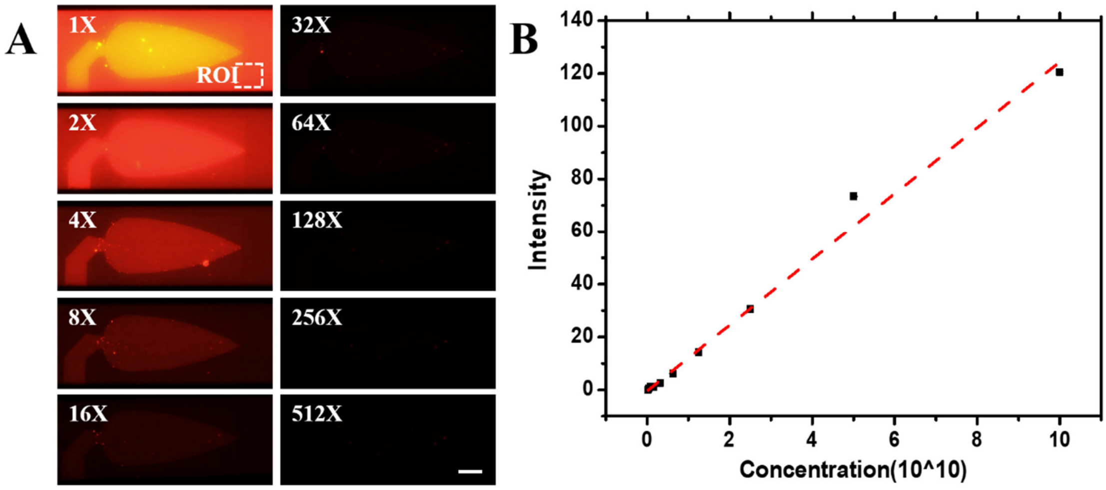

Fig. S9. Calibration curve of the concentration and fluorescence intensity of the nanoparticles. (A) Fluorescence images of the nanoparticles in the microfluidic device at various concentrations. The scale bar is 100 μm. (B) The calibration curve of the concentration and fluorescence intensity values. Each dot in the diagraph was calculated by the average value in the ROI from 10 discrete images. The concentration of origin sample was tested by NTA.

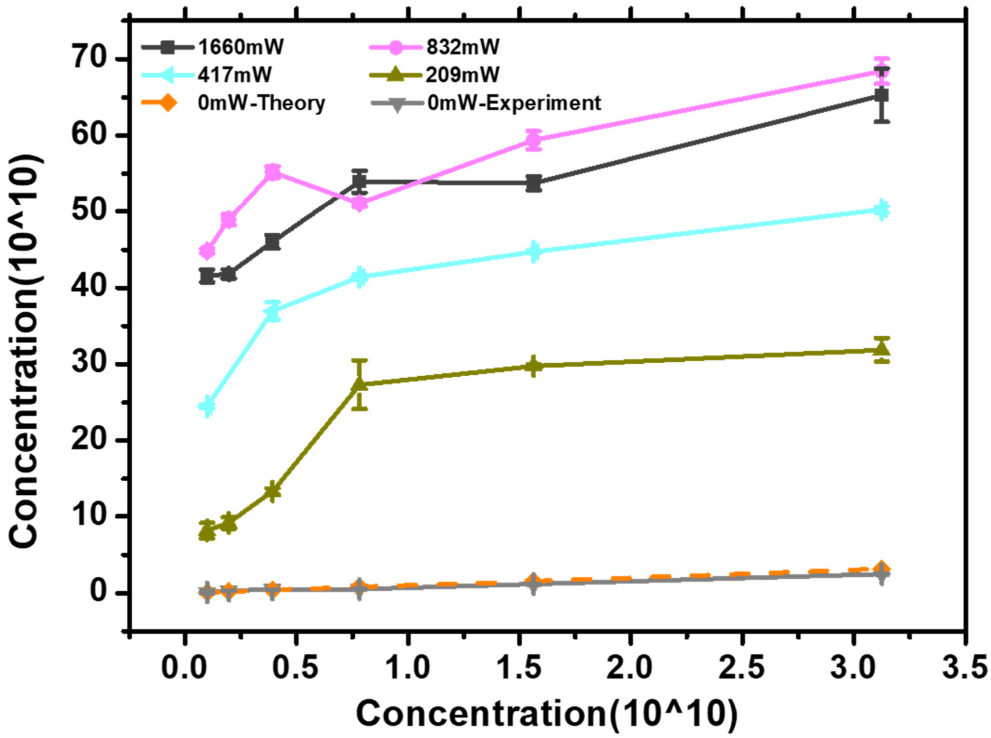

Fig. S10. In situ enrichment of nanoparticles. The relationship between the applied power and the concentration before and after in situ enrichment.

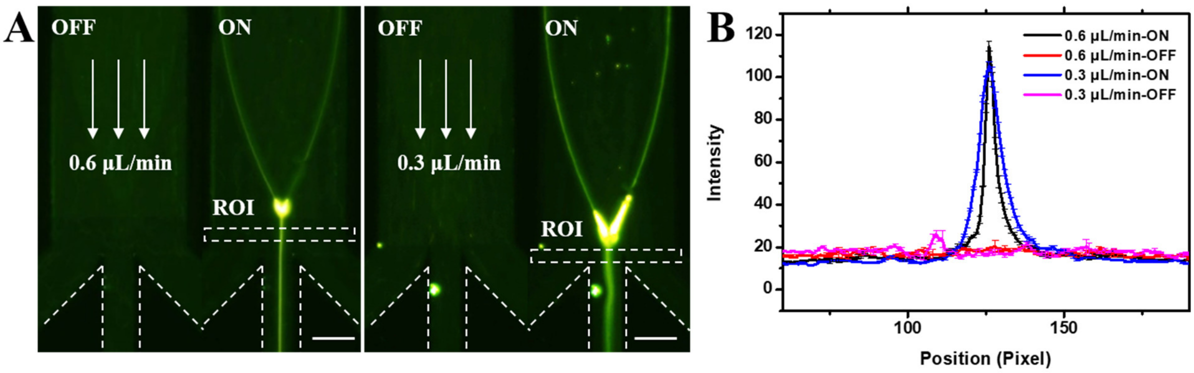

Fig. S11. Continuous focusing of 150-nm nanoparticles at different flow rates. (A) The fluorescence images of 150 nm PS nanoparticle focusing at flow rates of 0.6 and 0.3 μL/min and the applied power of 1660 mW. The flow direction is pointed by white arrows and the boundaries of outlets is marked by white dashed line. The regions of interesting (ROI) are highlighted by white dashed rectangles. The scale bars are 100 μm. (B) The fluorescent intensity of the images at different flow rates in the ROI.

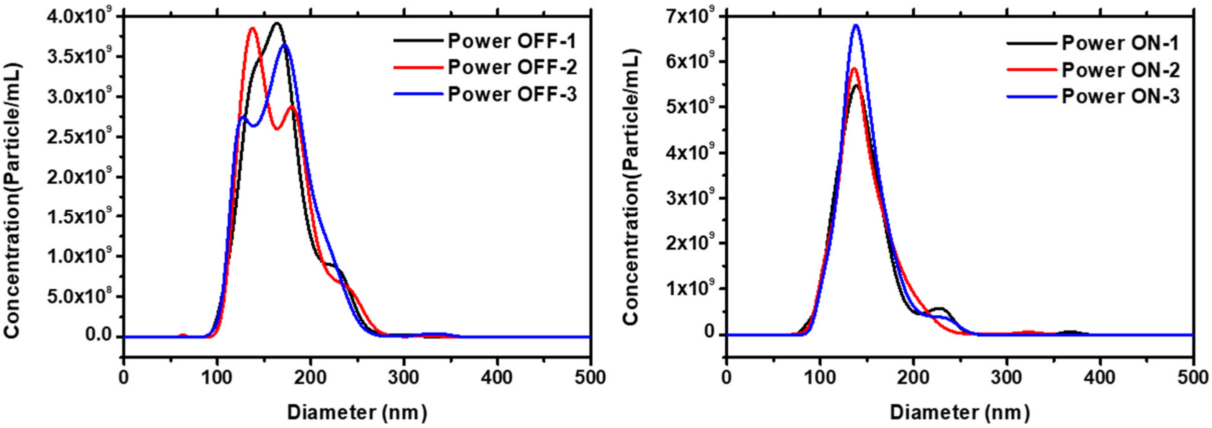

Fig. S12. The concentration and size distribution of EVs with/without purification tested by NTA.

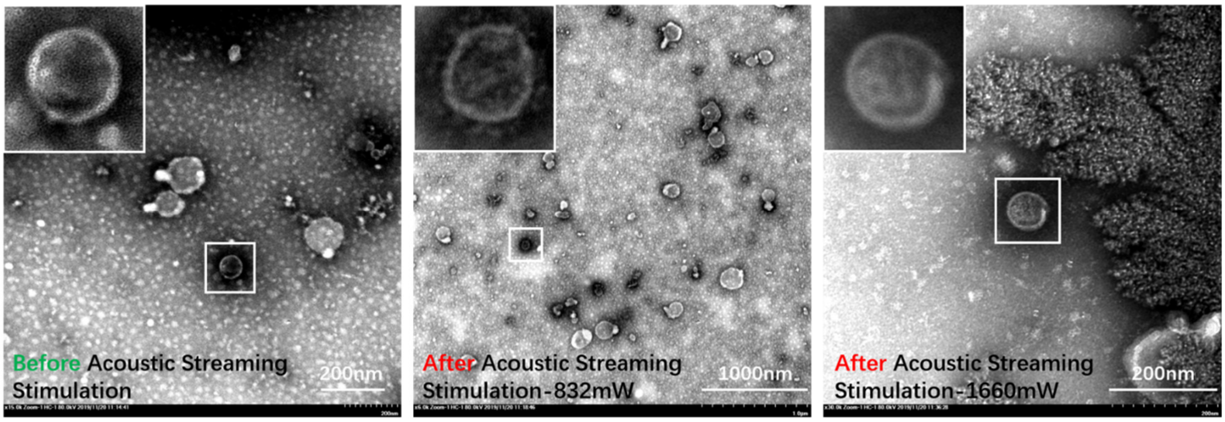

Fig. S13. Morphologies of exosomes before and after SteAS stimulation. TEM images of exosomes before and after stimulation at 832 mW and 1660 mW by stereo acoustic streaming. The height of the microfluidic channel was 50 μm. The flow rate was 0.8 μL/min.

Table S1: Comparison of different nanoparticle enrichment/focusing techniques

Method	Mode	Separation Marker	Limiting Size (Polystyrene)	Recovery Efficiency(%)	Throughput	Advantages	Disadvantages
Conventional methods							
Ultracentrifugation *(18, 21)*	Enrichment	Density, size	50-nm	2-80	3-12 h	Large processing volume	Expensive equipment, limitation of volume for each batch, agglomeration
Ultrafiltration *(18, 21)*	Enrichment	Size	200-nm	10-80	0.5-3 h	Relative high efficiency, easy to use	Clogging, bioparticles structure damage, protein aggregate
Microfluidics methods							
Immunoaffinity *(17, 27)*	Enrichment	Antigenic site	-	42-97	20 min	Low soluble protein contamination, eligible for specific exosomes	Expensive antibody, strict preservation conditions, additional washing step, hard to release, biased separation
Viscoelastic *(26, 31)*	Focusing	Size, shape	300-nm	~80	3.33 µL/min	Do not need external actuation	Requirement of elasticity enhancers, low throughput
Filtration *(20, 21, 22)*	Enrichment	Size, deformability	~20	96.5	120 µm/s	High recovery efficiency, high resolution	Clogging, hard to fabrication, hard to release, potential mechanical damage
Dielectrophoresis *(27, 32)*	Enrichment	Size, polarizability	50-nm	-	~30 min	Low soluble protein contamination	potential structural damage, low sample volume per batch, requirements for specific buffer
Thermophoresis *(10)*	Enrichment	Size	23-nm	-	10 min	High enrichment factor, rapid enrichment process	Hard to recovery, potential heating effect
Deterministic lateral displacement *(30)*	Focusing	Size	110-nm	-	0.1-0.2 nL/min	High sorting resolution, high biocompatibility	Clogging, time consuming processing (~60h)
Acoustofluidics *(21, 23, 27, 34)*	Enrichment Focusing	Size, acoustic contrast factor	110-nm 340-nm	- 82	1 min 4 µL/min	Biocompatibility, contactless, no requirement of additional reagent	Soluble protein contamination, relative low throughput
Acoustofluidic centrifuge *(49)*	Enrichment	Size, acoustic contrast factor	30-nm	80-86	~35 s	Simple configuration, high performance	Low sample volume per batch, potential evaporation issue
Virtual microchannel **(this work)**	Enrichment Focusing	Size, acoustic contrast factor	30-nm 150-nm	- 55-93	- 0.6-3 µL/min	Multifunction, high performance, biocompatibility, good compatibility with sample properties and concentrations	Relative low throughput, soluble protein contamination

Enrichment refers to a mode in which the target particles is enriched to a fixed location in continuous flow or batch of samples; Focusing refers to the mode in which the target particle is laterally displaced and focused in continuous flow. For batch mode processes, throughputs are reported in terms of the total time required to complete enrichment or separation; For continuous mode processes, throughputs are reported in terms of flow rates.

Movie S1. Vibration of GHz BAW device.

Movie S2. Nanoparticle enrichment in chamber.

Movie S3. Process of nanoparticle enrichment.

Movie S4. Section view of stereo acoustic streaming.

Movie S5. Height effect in nanoparticle enrichment.

Movie S6. Size effect in nanoparticle enrichment.

Movie S7. Enrichment and release of 100-nm PS nanoparticles.

Movie S8. Continuous focusing of 300-nm PS nanoparticles.

Movie S9. Continuous focusing of 200-nm, 150-nm and 100-nm PS nanoparticles.

Movie S10. Focusing-type separation of nanoparticles.

Movie S11. Exosome separation via virtual microchannel.